2012

Out-of-plane motion of a planar dielectric elastomer actuator with distributed stiffeners

William Lai
Iowa State University

Ashraf F. Bastawros
Iowa State University, bastaw@iastate.edu

Wei Hong
Iowa State University, whong@iastate.edu

Out-of-plane motion of a planar dielectric elastomer actuator with distributed stiffeners

Abstract
A new design for a multi-layer dielectric elastomer actuator, reinforced with periodic stiffeners is presented. The resulting actuator enables complex out-of- plane motion without the need of the elastomer membrane prestretch. An in situ optical imaging system is used to capture the complex deformation pattern and track the non-planar displacement and curvature under the applied voltage. The role of the stiffeners periodicity, φ, on the macroscopic actuator response is analyzed numerically utilizing ABAQUS finite element software. A user-material subroutine is developed to represent the elastomer deformation under the applied electric field. It is found that the actuator force-stroke characteristics can be greatly changed by varying φ, while maintaining the same overall actuator stiffness. The numerical results showed a band of localized deformation around the stiffeners. The refinement of the stiffener, φ, increases the total actuated volume within the span of the actuator, and thereby the macroscopic actuator stroke. The stored elastic strain energy within the actuator is also increased. φ might be further refined down to the actuator sheet thickness, wherein the localized deformation bands overlaps. This is the practical limit of the stiffeners spacing to achieve the largest macroscopic actuator stroke. The developed experimental and modeling framework would enable the exploitation and optimization of different actuator designs to achieve a preset load-stroke characteristic.

Keywords
Electroactive polymer, dielectric elastomer, actuator, bending, stiffener reinforcement

Disciplines
Aerospace Engineering

Comments
This article is from *Proceedings of SPIE - The International Society for Optical Engineering* 8340 (2012): 834011, doi: 10.1117/12.917494. Posted with permission.

Out-of-Plane Motion of a Planar Dielectric Elastomer Actuator with Distributed Stiffeners

William Lai*[a], Ashraf F. Bastawros[a], Wei Hong[a]
[a]Department of Aerospace Engineering, Iowa State University, Ames, IA USA 50011-2271

ABSTRACT

A new design for a multi-layer dielectric elastomer actuator, reinforced with periodic stiffeners is presented. The resulting actuator enables complex out-of- plane motion without the need of the elastomer membrane prestretch. An in situ optical imaging system is used to capture the complex deformation pattern and track the non-planar displacement and curvature under the applied voltage. The role of the stiffeners periodicity, φ, on the macroscopic actuator response is analyzed numerically utilizing ABAQUS finite element software. A user-material subroutine is developed to represent the elastomer deformation under the applied electric field. It is found that the actuator force-stroke characteristics can be greatly changed by varying φ, while maintaining the same overall actuator stiffness. The numerical results showed a band of localized deformation around the stiffeners. The refinement of the stiffener, φ, increases the total actuated volume within the span of the actuator, and thereby the macroscopic actuator stroke. The stored elastic strain energy within the actuator is also increased. φ might be further refined down to the actuator sheet thickness, wherein the localized deformation bands overlaps. This is the practical limit of the stiffeners spacing to achieve the largest macroscopic actuator stroke. The developed experimental and modeling framework would enable the exploitation and optimization of different actuator designs to achieve a preset load-stroke characteristic.

Keywords: Electroactive polymer, dielectric elastomer, actuator, bending, stiffener reinforcement

1. INTRODUCTION

Electroactive polymers (EAPs), one of the widely studied smart materials, are polymers that can induce deformation under electrical stimulation. EAPs exhibit unique characteristics, such as lightweight, considerable large stroke, and acceptable response time (in millisecond) [1-3]. From the EAPs family, dielectric elastomers have been especially considered due to their high strain, comparably short response time, low cost, and high electromechanical coupling efficiency [4-6]. Dielectric elastomer actuators (DEAs) are made of nearly incompressible compliant dielectric elastomer membranes sandwiched between compliant electrodes to form dynamic capacitors. When electric field is applied across the electrodes, the columbic force generates a stress called Maxwell stress [7] that attracts the electrodes together, squeezing the sandwiched dielectric elastomer layer. As a result, a large in-plane expansion of DEA commences due to elastomer incompressibility.

It has been shown that membrane prestretch greatly improves the DEAs performance [8, 9]. However, the prestretch is accompanied by several technical setbacks. A supporting skeletal frame is required to sustain the prestretched membrane and thereby reducing the actuator stroke-to-weight ratio [10, 11]. The total actuation strain is limited to the extent of the prestretch, otherwise the membrane would wrinkle. Furthermore, non-uniform prestretch and stress relaxation may affect subsequent actuation [12]. Our preliminary work showed that the actuation strain of DEAs is controlled by the biaxial prestretch ratio [13], the membrane response could be greatly biased, wherein direction with the larger prestretch tends to induce lower actuation strain. It has been also shown that stacking planar expanding actuator and inactive layer together can induce bending and non-planar movement [10]. Therefore, the goal of the current study is to explore the utilization of planar stiffeners with DEAs to avert the need for membrane prestretch.

In this work, our strategy is to fabricate laminates of dielectric elastomers with stiffeners having different periodicity, while maintaining the same macroscopic laminate stiffness. These stiffeners constrain the planar expansion along their

*william7@iastate.edu; phone +1 515-294-0085

Electroactive Polymer Actuators and Devices (EAPAD) 2012, edited by Yoseph Bar-Cohen,
Proc. of SPIE Vol. 8340, 834011 · © 2012 SPIE · CCC code: 0277-786X/12/$18 · doi: 10.1117/12.917494

axes, inducing a deformation gradient within the thickness of the DEAs laminate. The change of the stiffener periodicity, φ, would provide different load-stroke characteristics, for the same actuator stiffness. An in situ optical imaging system is utilized to track the deformation pattern and curvature of DEA laminate with different number of active layers and stiffener periodicity. A user-material subroutine, employing Neo-Hookean constitutive description and coupling with applied electric field is developed within the ABAQUS (Ver. 6.10) commercial finite element package. The numerical framework is used to understand the deformation mechanisms in the laminated actuator structure. The role of φ on the macroscopic actuator response is also addressed.

2. ACTUATOR MATERIAL SELECTION

Several dielectric elastomers and silicon along with compliant electrodes have suggested in literatures [13-16]. Here, in addition to acceptable performance and geometric requirements for our unique laminated actuator, we also consider materials availability and ease of prototype fabrication and assembly of different flexible actuator configurations.

A 50μm thick dielectric elastomer, 3M VHB (F9460PC) transfer tapes, were employed in this study. The tape has acceptable electro-mechanical coupling properties as well as adhesive surface to retain the flexible electrode, stiffeners and enable stacking of multiple layers. The 3M VHB tapes has been utilized in many DEAs prototypes [1, 6, 10, 11, 16], due to their high dielectric constant (4.7), low shear modulus (~0.042MPa), and for thicker films; great ability to withstand very large axial stretch up to 6 times [3, 17]. Thinner films are more desirable in free standing applications to limit the maximum applied voltage required for the desired electric field (electric potential per thickness). The resulting Maxwell stress is given by,

$$\sigma_{Maxwell} = -\epsilon\epsilon_0 E^2 \tag{1}$$

where ϵ, ϵ_0, and E are dielectric constant, permittivity and applied electric field respectively. The driving force in the actuator is proportional to the electric field. To maximize the actuator response under the same applied voltage, either a thinner laminate thickness gauge or laminate pre stretch should be utilized to increase the effective electric field.

Carbon black powders (Super C65, TIMCAL Inc., USA) was employed to form compliant electrodes. In general, carbon-based powders (alone or suspended in oil or grease) have outstanding electrical conductivity while providing great compliance and tolerance to large strains. In this study, the selected carbon black provides: (i) ease of handling compared to grease, (ii) remains dry and does not smear or squeeze out, (iii) better packing (percolation) and uniform area coverage, especially during actuation, and (iv) better structural adhesion and integration to multiple layers.

The stiffeners were fabricated from 3M Magic scotch tapes (~62.5μm thick). Such tape has good electrical insulation, about the same thickness and Young's modulus of 3.2GPa which is several orders of magnitude of the the DEA layer. These attributes would make the stiffeners, electrically in-active, constrain the DEA planar deformation and enable bending actuation.

3. FABRICATION PROCEDURE

The fabricated device had a square shape of 25×25mm. It contained an active area in the middle with 22×22mm and inactive border of about 1.5mm around the edge for sealing and preventing circuit shorting (Figure 1a). A window mask was used to define the electrode area. The carbon black powder was uniformly brushed over the window mask. Narrow strips of Aluminum foils were attached to the electrode edge to form the external terminals of the actuator. Finally, a dummy VHB tap layer was applied on the stack as a cover. The sequence was repeated for multiple stack modules. The aluminum terminal points were alternated to separate positive and negative electrode and fabricate multi-layer structure. As an example, sketches of 2 (which is the minimum stack of basic DEA design), 3, and 4-stack structure are shown in Figure 2. For the stiffener part, 3M Magic scotch tapes were cut into long-narrow shape with 3mm width and attached on the surface of the DEA laminates stack (Figure 1b).

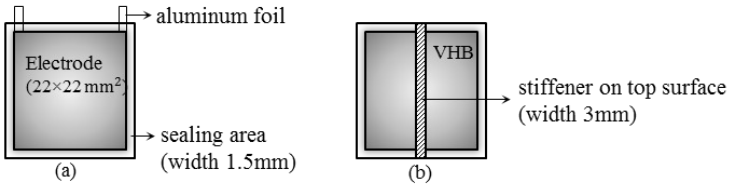

Figure 1. Sketches of DEA samples. (a) Top view of unit-cell DEA structure and its measurement with (b) single strip configuration stiffener in the middle on the surface.

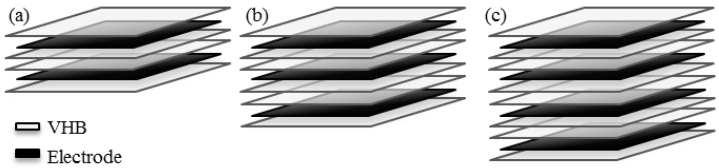

Figure 2. Sketches of DEA samples fabrication with side view of different stack configurations. (a) 2-stack (b) 3-stack (c) 4-stack.

4. EXPERIMENTS

In the experiments, DEA samples were hung from the attachment electrodes and connected to the high voltage circuit terminal [18] with and applied maximum voltages range of 2-3.2kV by utilizing a DC-DC voltage converter (Q-80, EMCO Inc.). The converter has a high DC voltage linear amplifier range of 0 – 8kV output for 0–5V input. The actuator movements were captured by high-resolution CCD camera (2448×2048 pixel, Grasshopper, Point Grey Inc.) for out-of-plane displacement and curvature analysis. The deformed configuration sequence of a 4-stack actuator is shown in Figure 3 under an applied voltage range of 0-3.2kV.

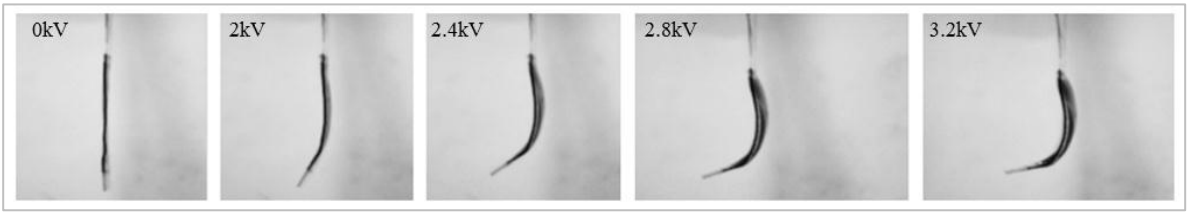

Figure 3. Deformed shape of a 4-stack configuration actuator under applied voltage range of 0-3.2kV

5. SIMULATION

The actuation response of the DEAs actuator was numerically studied by the finite element method. A user material (UMAT) subroutine was developed within the ABAQUS commercial finite element software. A Neo-Hookean material model was employed to couple the applied electric field with the actuator mechanical deformation. The electric field was imposed similar to an external thermal field with the resulting thermal strains. The incompressible Neo-Hookean material model was utilized due to its simplistic representation (compared to Ogden model) and coupling with the external field. In this model, the strain energy density, W is given in terms of a single material parameter, μ, the shear modulus and the principal stretches, λ_i;

$$W = \frac{\mu}{2}\left(\lambda_1^2 + \lambda_2^2 + \lambda_3^2 - 3\right); \quad \lambda_1\lambda_2\lambda_3 = 1 \tag{2}$$

The Cauchy stress differences are given in terms of the principal stretches λ_i by

$$\sigma_i - \sigma_j = \lambda_i \frac{\partial W}{\partial \lambda_i} - \lambda_j \frac{\partial W}{\partial \lambda_j} = \mu\left(\lambda_i^2 - \lambda_j^2\right) \tag{3}$$

A 3D geometric model for the laminated cantilever was constructed. One edge was completely anchored, and the other edge was either left free to move, or constrained in the direction normal to the plane of the actuator to derive the force-stroke characteristics A hybrid 20-node quadratic brick element is used in constructing each individual layer. The surface-based tie constraint was utilized to link the individual layers to form the laminated actuator.

6. ACTUATOR PERFORMANCE

The bending curvatures were calculated from the experimentaly recorded images under different activation voltages, and for different stack configurations. The result of a single layer stack was used to calibrate the FEM numerical results (i.e., fix the proportionality constant for the electric-mechanical coupling). Once established, the model was used to investigate the deformation mechanisms and the domain of influence of each stiffener on the constrained DEAs laminates under the applied electric field. The role of the stiffener periodicity on the macroscopic response of the actuator was also investigated at constant actuator stiffness.

6.1 Measured actuator response with a single stiffener configuration

The experimentally evaluated bending curvatures under different level of applied voltage are shown in Figure 4. The curvature of the entire actuator was assumed to be approximately uniform over the entore active span. Curvature measurements were conforming to the active span only. The experimental results showes that the stack curvature increased with the number of active layers. Such trend in active materials is different than the behavior of simple beam bending, wherein thicker beam would bend less under the same applied load. It is convinced that the increase of the number of active stacks in the actuator configuration will increase the driving forces that have to remain in balance with the forces generated within the stiffening layer. In addition, the role of the inactive cover layer on each side of the stack has to be considered. In our design, samples are covered with an additional VHB layer on each of the top and bottom surfaces for protection of the electrodes (Figure 2). As a result, the more stacks we have, the less effect we would get from them as they are being diluted. A predictive analytical model, accounting for these detials and utilizing the Timoshenko's analysis of bi-material can be found in [13].

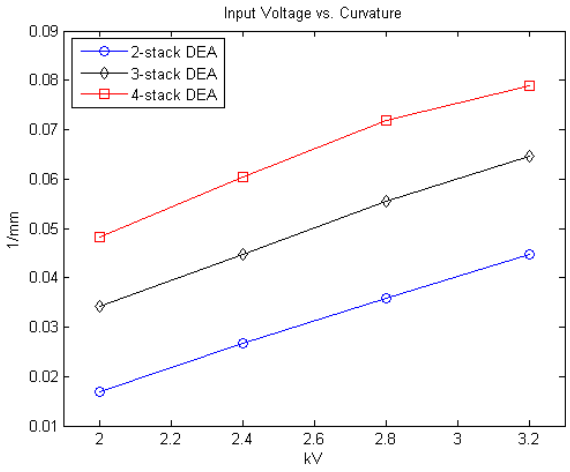

Figure 4. The experimentally evaluated bending curvatures for different stack configurations of actuators with single stiffener under a range of applied voltage potential.

6.2 Role of stiffener periodicity

Several configurations have been examined numerically as shown in Figure 5. The total stiffener covering area is the same to maintain the overall actuator stiffness. However the stiffener width was divided and spread with different periodicity, φ. The simulation results showed that the distribution of stiffeners will significantly influence the macroscopic bending response as depicted in Figure 6. As the stiffener periodicity φ, increases, the stroke characteristics changes with much higher stroke were observed.

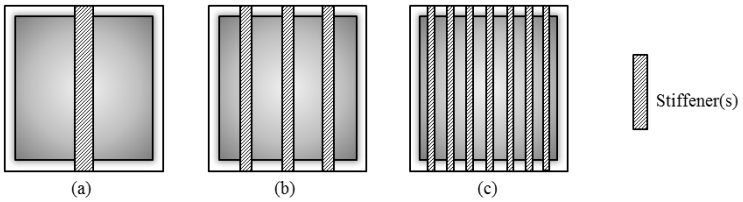

Figure 5. Sketches of stiffeners periodicity variation by splitting the stiffener(s) into distrusted segments while maintaining the total stiffener width to keep the entire stiffness. (a) 1 segment (φ=1), (b) 3 segment (φ=3), (c) 7 segment (φ=7).

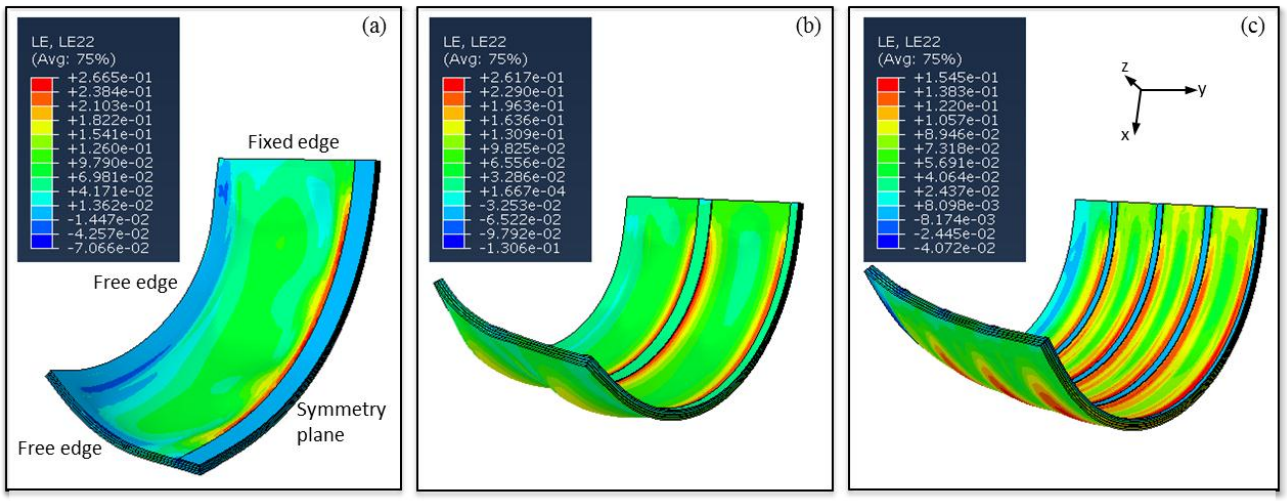

Figure 6. FEM results of the in-plane strain along the stiffeners direction, shown on the deformed mesh for different φ; (a) φ=1, (b) φ=3, (c) φ=7. The total actuated volume within the span of the actuator increases with the refinement of the stiffener, φ.

The distribution of the in-plan strain component, normal to the stiffeners direction is shown also as false color on Figure 6. It clearly shows the existence of a localized deformation band, neighboring the stiffener. As the number of stiffeners increases, the activated volume of the bands relative to the total volume of the actuator increases. Moreover, the free edge effect can be seen by showing no activities. By increasing φ, the free edge domain is further reduced, contributing to additional actiovated volume. The effect of the stiffners can be further understood by examining the total stored elastic strain energy shown in Figure 7 as a function of the stiffeners periodicity. The elastic strain energy increases by 150% by spliting a single stiffener to three stiffeners configuration. Then it increases by almost another 100% by splitting to seven stiffeners configuration. This trend indicate that the existence of a boundary layer next to the stiffeners, increases the total actuated volume and thereby the stored elastic strain energy and the macroscopic response. However, further refinement would not result in further increase of the stroke. These localized bands start to overlap, when the spacing between the stiffeners reaches the laminate thickness. Further refinement would not have any effect on the macroscopic response. The direct outcome of such finding is the design of a tunable force-stroke characteristics for actuator with eth

same overall stiffness. Moreover, one could also stipulate that the increase of the stored elastic strain energy is an indication of an increase of the mechanical coupling conversion efficiency, as higher level of the applied electric potential can be converted to elastic potential and thereby to possible external work. The details of conversion efficiency and the possible increase in the mechanical work are under further investigation.

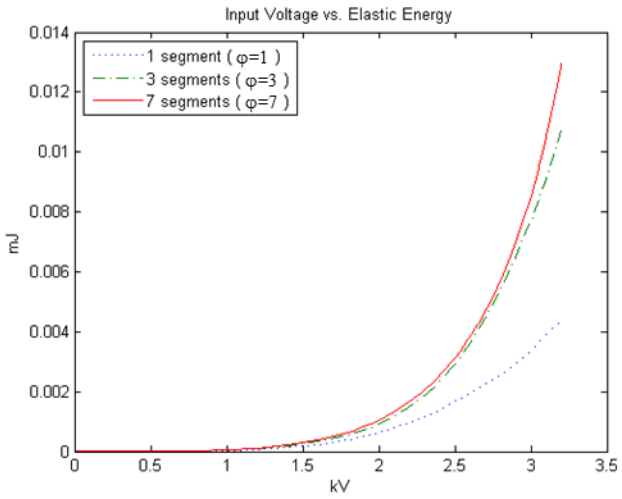

Figure 7. The FEM results of the variation of the elastic strain energy with splitting stiffeners into narrower segments.

7. CONCLUSION

A new design of a free standing planar actuator based on multi-layer dielectric elastomer actuator with geometrically confining reinforcements capable of out of plan deformation is presented. The performance of the actuator is experimentally evaluated by an in situ imaging system and numerically calibrated by an established finite element material model framework coupling the applied electric field to the resulting deformation. The role of the stiffener periodicity on the overall actuator performance is presented. A localized deformation band was found, adjacent to the stiffeners and is responsible for the observed performance enhancements.The results show the promise of developing the actuator configuration to deliver different force-stroke characteristics at a given overall actuator stiffness. The presented experiment-numerical framework would enable further development of similar actuators at prescribed performance characteristics.

ACKNOWLEDGEMENT

This work is supported by U.S. Army Research Office under Award No W911NF-10-1-0296.

REFERENCES

[1] Bar-Cohen, Y., Electroactive Polymer (EAP) Actuators as Artificial Muscle: : Reality, Potential, and Challengesnd edition, Bellingham, WA: SPIE, 2004.

[2] Madden, J.D.W., Vandesteeg, N.A., Anquetil, P.A., Madden, P.G.A., Takshi, A., Pytel, R.Z., Lafontaine, S.R., Wieringa, P.A., and Hunter, I.W., "Artificial muscle technology: physical principles and naval prospects," *IEEE J. Ocean. Eng.*, vol. 29, no. 3, pp. 706-728, (2004).

[3] Kim, K. J. and Tadokoro, S., Electroactive Polymers for Robotic Applications: Artificial Muscles and Sensors, London, UK: Springer, (2007).

[4] Ashley, S., "Artificial muscles," *Scientific American,* p. 52–59, October (2003).

[5] Kornbluh, R., Pelrine, R., and Pei, Q., "Dielectric elastomer produces strain of 380%," *EAP Newsletter, 2(2),* p. 10–11, (2002).

[6] Pelrine, R.; Kornbluh, R.; Joseph, J.; Heydt, R., "High-field deformation of elastomeric dielectrics for actuators," *Materials Science & Engineering C,* vol. 11, no. 2, p. 89–100, (2000).

[7] Roentgen, W. C., "About the Changes in Shape and Volume of Dielectrics Caused by Electricity," *Annual Physics and Chemistry Series,* Vols. 11, Section III, (1880).

[8] Pelrine, R., Kornbluh, R., Pei, Q., and Joseph, J., "High-speed electrically actuated elastomers with strain greater than 100%," *Science,* vol. 287, p. 836–839, (2000).

[9] Zhao, X., Suo, Z., "Theory of dielectric elastomers capable of giant deformation of actuation," *Phys. Rev. Lett.,* Vols. 104, 178302, (2010).

[10] Kornbluh, R., Perine, R., Pei, Q., Heydt, R., Stanford, S, Oh, S., and Eckerle, J., "Electroelastomer: application of dielectric elastomer transducers for actuation, generation and smart structures," *Proc. SPIE Int. Soc. Opt. Eng. 4698,* p. 254–270, (2002).

[11] Petralia, M. T. and Wood R. J., "Fabrication and analysis of dielectric-elastomer minimum-energy structures for highly-deformable soft robotic systems," Intelligent Robots and Systems (IROS), 2010 IEEE/RSJ International Conference on , pp. 2357 - 2363 , (2010).

[12] Sommer-Larsen, P., Kofod, G., Shridhar, M. H., Benslimane, M., and Gravesen, P., "Performance of dielectric elastomer actuators and materials," *Proc. SPIE Int. Soc. Opt. Eng.4695,* p. 158–166, (2002).

[13] Lai, W., "Characteristics of Dielectric Elastomers and Fabrication of Dielectric Elastomer Actuators for Artificial Muscle Applications, , M.S. thesis," Iowa State University, (2011).

[14] Carpi, F., Chiarelli, P., Mazzoldi, A., and De Rossi, D., "Electromechanical characterisation of dielectric elastomer planar actuators: comparative evaluation of different electrode materials and different counterloads," *Sensors & Actuators: A. Physical,* vol. 107, p. 85–95, (2003).

[15] Benslimane, M.Y., Kiil, H.E., and Tryson, M.J., "Dielectric electroactive polymer push actuators: performance and challenges," *Polymer International,* vol. 59, no. 3, p. 415–412, (2010).

[16] Gallone, G., Galantini, F., and Carpi, F., "Perspectives for new dielectric elastomers with improved electromechanical actuation performance: Composites versus blends," *Polymer International,* vol. 59, no. 3, p. 400–406, (2010).

[17] Kofod, G., "Dielectric elastomer actuators, Ph.D. thesis," The Technical University of Denmark, (2001).

[18] Wingert, A, Lichter, M. D. Dubowsky, S., "On the Design of Large Degree-of-Freedom Digital Mechatronic Devices Based on Bistable Dielectric Elastomer Actuators," *IEEE/ASME Transactions on Mechatronics,* vol. 11, no. 4, pp. 448-456, (2006).